2 Theory and Methods

2.1 Cold Molecules in a Collision Free Environment: Molecular Beams

In order to obtain molecules that are isolated from each other and distributed over a small number of internal states only, the application of a supersonic expansion of a gas through a nozzle into a vacuum chamber leading to the formation of a so called molecular beam is an effective method frequently used in the field of molecular dynamics. The first to use effusive beams was Otto Stern in 1920[1], making the famous Stern Gerlach experiment possible. At that time, having particles in a collision free environment was the most desired feature which was obtained in this way. Effusive beams are formed if the ratio of the mean free path of the molecules and the diameter of the nozzle orifice is greater than 1, i.e. under the pressure and temperature used in the experiment. This can be conceived by imagining that only one molecule at a time randomly hits the area of the nozzle orifice and thus, energy and momentum are conserved and the temperature is not altered. If the ratio is larger than one, the molecules come out as a jet and a region of gas dynamic flow in and just behind the nozzle is formed where collisions occur. This leads to a more collimated beam, i.e. the angular distribution is rather $\cos^2(\theta)$ than $\cos(\theta)$ as in the case of effusive beams. It is also cooled down with respect to the translation in the direction of the beam propagation and the internal degrees of freedom, since the thermal energy is transferred into kinetic energy of the beam.[2] The local Mach number M can become larger than 1 at the nozzle orifice if the ratio P_{gas}/P_{vac} is greater than $G = ((\kappa+1)/2)^{\kappa/(\kappa-1)}$, where G is smaller than 2.1 for most gases (κ is the adiabatic exponent).[3] Therefore this type of expansion is also termed supersonic. Depending on the background pressure on the vacuum side, two general types of molecular beam sources can be distinguished. For relatively high pressures, the supersonic beam hits the background gas with a higher speed than the background gas can react to the perturbation travelling at the local speed of sound. The result is a shock wave structure with the dimensions of the local mean free path[4] and huge pressure and temperature gradients. Since this region shields the beam from the surrounding gas – the better, the higher the mass of the gas is – this effect can also be used to separate isotopes.[5] This type of beam source is termed a Campargue source. A sketch of the circumstance for Campargue sources is shown in figure 1. Inside the so called barrel shock structure the flow is unhindered by the background pressure. Therefore, this zone is called the zone of silence. The barrel shocks lead to constriction of the beam and at the so called Mach disc, M assumes numbers smaller than one.

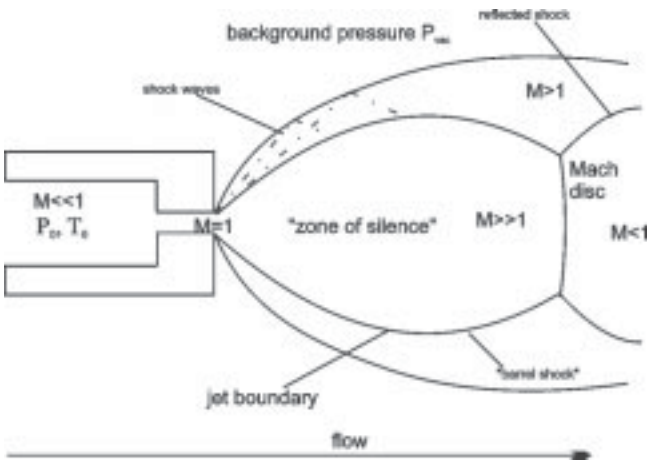

FIG. 1: Molecular beam structure for a Campargue source

Miller[3] points out that for very small pressures (e.g. 10^{-3} mbar) the mean free path becomes too large for the shock wave structure to be significant. Here a smooth transition from a gas dynamic flow to the molecular flow is achieved. Beam sources like this are called Fenn-type sources.[6] All beam sources in this study are of this latter type.

In order to achieve also cooling in the transversal direction, a skimmer can be used to select only those molecules travelling on the beam center line. The position to place the skimmer is behind the Mach disc for a Campargue source and behind the so called quitting surface (Beijerinck and Verster (1981)).[3] This process is called geometric cooling. Since the density in the beam decreases as $1/d^2$ where d is the distance to the orifice, some of the measurements in this work have been conducted without a skimmer in order to get nearer to the nozzle. Since it is desirable to have as little gas as possible in the vacuum chamber, pulsed nozzles will be used for this. The characterization of the molecular beam with respect to the temperatures for the rational and translational degrees of freedom has been described earlier.[7,8]

2.2 Molecular Spectroscopy

Experiments in reaction dynamics contain much more information if they are carried out specific to the quantum state of the reactants and products. If the state of the first is not prepared e.g. by absorption of an appropriate photon, their state distribution assumes only considerable values for the lowest rotational levels of the vibronic ground state if the molecules have been cooled in a molecular beam expansion. Its influence is usually of minor importance and is therefore neglected. The product state distribution is a sensitive probe for

the potential energy surface(s) that govern the dynamics (see chapters 4 and 5). This information can be gathered using spectroscopy with narrowband light sources (i.e. lasers in most cases today).

Since reaction products in this thesis are detected as ions formed by resonance enhanced multi photon ionization (REMPI[m+n]), a short introduction to electronic spectroscopy follows in the next paragraphs. In a REMPI[m+n] process, molecules are first excited to a stationary state by m photons and then ionized by n additional photons.

According to the Born-Oppenheimer approximation, the molecular wave function can be written as a product of a part describing the movements of the nuclei and the electronic wave function at fixed positions of the nuclei. Under this assumption, the time independent Schrödinger equation can be solved at fixed positions of the nuclei which leads to the concept of adiabatic potential energy surfaces describing the energy eigenvalue of the solution as a function of the positions of the nuclei.

$$\psi(\vec{r}_e, \vec{R}) = \varphi(\vec{R}) \cdot \phi(\vec{r}_e; \vec{R}) \tag{1}$$

Equation 1 expresses the fact that the light electrons move fast in the electronic potential of the much slower – or ideally stationary – nuclei. An extension of this is known as the Franck Condon principle for electronic transitions which also assumes that the absorption of a photon happens instantaneously and the nuclei have no time to move while the electronic configuration is changed. These transitions are also called perpendicular since they connect two electronic levels with a straight parallel to the energy axis (i.e. perpendicular to all independent coordinates) in a plot of the potential as a function of the nuclear coordinates. Generally speaking, the interaction of a quantum system having two states with a plane electromagnetic wave $E_0 \cdot \cos(kx-\omega t)$ can be described as follows: placing the molecule at $x = 0$ and letting the wave be polarized in the z direction (i.e. $E_0 = (0,0,E_{0,z})$) , the potential energy to be added to the Hamiltonian of the unperturbed system is $V_E = eE_{0,z}z\cos(\omega t)$. Application of perturbation theory leads to matrix elements of the form:

$$H_{ij} = \left\langle \psi_i^* \middle| eE_{0,z} z \middle| \psi_j \right\rangle \cos(\omega t) = E_{0,z} \mu_{ij} \cos(\omega t) \tag{2}$$

The indices i and j denote the two states and μ_{ij} is usually 0 for $i = j$ and otherwise the transition dipole moment. The transition dipole moment μ_{12} can be chosen real and equal to μ_{21} and is connected with the Rabi frequency through $\omega_{Ra} = 1/(2\hbar)E_{0,z} \cdot \mu_{12}$.

The total wave function is then:

$$\Psi = c_1\left|\psi_1\right\rangle + c_2\left|\psi_2\right\rangle; c_1 = \cos(\omega_{Ra}t)e^{-iE_1t/\hbar};\ c_2 = -i\sin(\omega_{Ra}t)e^{-iE_2t/\hbar} \quad (3)$$

Taking the absolute value of equation 3, one sees that the population of the two states is oscillating with the Rabi frequency and the excited state 2 is being populated completely after $t = \pi/(2\omega_{Ra})$. This means that the transition dipole moment – for dipole transitions - is the property to be assessed if one wants to decide whether a transition between electronic states is possible. Since the molecular wavefunction factors according to equation 1, the matrix elements in equ. 2 can be treated independently for electronic and nuclear coordinates. For the matrix element H_{ij} to be non zero, all factors for the electronic part and the rotational and vibrational degrees of freedom have to non-zero. All this leads to selection rules reflecting the symmetry of the molecule and detailed descriptions can be found in references 9-13.

The details of the excitation can be found in the angular distribution of the molecular frame if polarized light has been used. This is directly connected to the conservation of angular momentum in quantum mechanics. E.g. the angular distribution P(θ) of the molecular frame after an excitation from a state having the total angular momentum J'' with all M'' substates equally populated to a final state with quantum numbers J and M by linearly polarized light ($j_{photon} = 1$, $m_{photon} = 0$) can be described by:

$$P_J(\theta) = \sum_{M''}\left\langle J''M'',10\middle|JM\right\rangle^2\left|Y_{JM}(\theta,\varphi)\right|^2 \quad (4)$$

Y_{JM} denotes a spherical harmonic and the factor in front of it is a Clebsch-Gordan coefficient for the angular momenta involved. This can be cast into the form:

$$P_J(\theta) = 1/4\pi\cdot(1 + A_0(J)P_2(\cos(\theta))) \quad (5)$$

Here P_2 is the second Legendre polynomial and $A_0(J)$ is the so called alignment parameter that ranges from -1 to 2 and becomes ½ for $J\rightarrow\infty$. A detailed description of quantum mechanical angular momentum algebra can be found in reference 14.

If the final state of an electronic excitation is repulsive in one or more coordinates, the process leads to the fragmentation of the molecule and the spatial velocity distribution of the fragments reflects the dynamics of the process. In this case the angular distribution of the photo fragments can be described analogously to equation 5:

$$P(\theta) = 1/4\pi\cdot(1 + \beta P_2(\cos(\theta))) \quad (6)$$

Here the so called β–parameter is given by the direction of the transition dipole in the molecular frame by $\beta = 2P_2(\cos(\theta_{v\mu}))$, where $\theta_{v\mu}$ denotes the polar angle between the recoil direction of the fragments and the transition dipole moment. E.g. in a diatomic molecule, β depends on the change of the quantum number Ω, the projection of the total electronic angular momentum on the internuclear axis. For $\Delta\Omega = 0$, $\beta = 2$ and the transition dipole lies along the internuclear axis. The angular distribution is therefore $\cos^2(\theta)$. For $\Delta\Omega = \pm 1$, $\beta = -1$ and the transition dipole is perpendicular to the internuclear axis, resulting in a $\sin^2(\theta)$ fragment distribution.

After the excitation, the molecule does not have to stay on its adiabatic potential but can also change the potential energy surface in a non-adiabatic transition. The transition probability can be understood by the simple Landau-Zener Model[15]:

$$P_{na} = e^{-2\pi\omega_{12}\tau_d} \tag{7}$$

Here, $\omega_{12} = |H_{12}|/\hbar$ and $\tau_d = |H_{12}|/(v|F_{12}|)$, with v as the speed with which the point of the non-adiabatic transition is approached and $F_{12} = F_1 - F_2$, the difference of the slopes of the two energy surfaces at the crossing. It reflects that the electronic rearrangement is facilitated the faster the nuclei are moving or the smaller the energy gap between them is – both promoting the Born-Oppenheimer breakdown. If the first potential is not dissociative one speaks of a predissociation which results in broadening of the absorption line according to the lifetime of the state.

2.3 Reaction Dynamics: Modeling the Angular Distribution of a Photoinitiated Bimolecular Reaction

In order to achieve the goal of a universal procedure for measuring the quantum state selected differential cross section of a bimolecular photoinitiated chemical reaction in only one molecular beam – thus having the advantage of high number densities of both reactants - a realistic model of the experimental circumstances has to be set up. This section shall serve as an introduction to the general set of terms and problems as well as a detailed description of the reaction model that will be used in the analysis in chapter 4.2.

The concept of the scattering cross section derives from the Lambert-Beer law which states that the attenuation dN of a particle beam in the interval $dz = vdt$ of its path is given by the number density of the target gas N_t, the number density of the incident beam N and the mutual

cross section of the two colliding particles σ. The situation for colliding hard spheres is depicted in figure 2.

$$dN = N_t \sigma N dz = N_t \sigma(v_{rel}) N v_{rel} dt \tag{8}$$

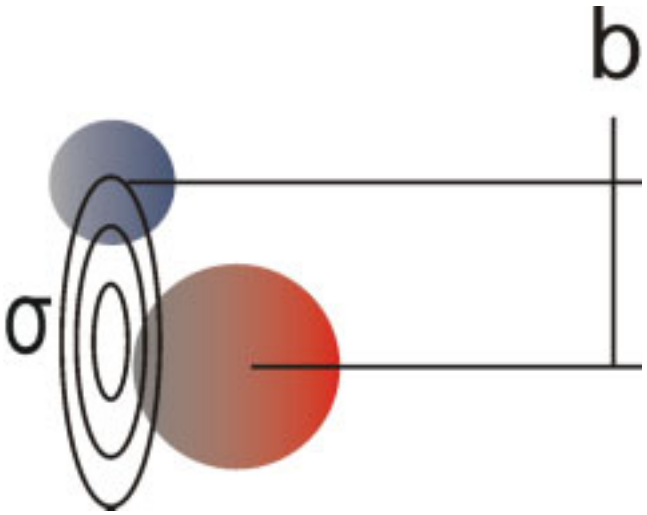

FIG. 2: Scattering cross section for hard spheres

Here the classical impact parameter b has also been introduced which is defined as the perpendicular component of the vector connecting the centers of mass of the two particles prior to the collision. In the case of colliding hard spheres, the scattering cross section σ is simply given by πb^2_{max} and is independent of the speed of the collision v_{rel}. Since molecules are no hard spheres, the interaction potential is not a step function but something else and a transfer of the collision energy into internal energy of the particles or vice versa can happen. This leads to a dependence of σ on the kinetic energy of the scattered particles and the form of the potential determines the angular distribution after the collision. The total scattering cross section can thus be written as:

$$\sigma = \int_0^{\infty}\int_0^{\pi} \sigma_d(\theta, E_{kin}) \sin(\theta) d\theta dE_{kin} \tag{9}$$

σ_d is the differential cross section $\partial^2\sigma/(\partial\cos(\theta)\partial(E_{kin}))$ and θ the scattering angle. The reaction cross section σ_r is then the fraction of the scattering cross section leading to a chemical reaction $\sigma = \sigma_{r+}\sigma_{nr}$ (nr: no reaction). Note that molecules are not spherical and therefore the cross section depends also on the orientation of the collision partners. Although this effect is averaged out for non-reactive scattering if the reactants are not aligned, in reactive scattering some of the information about orientation effects might be conserved in the averaged differential cross section. To conceive this, imagine a reaction like S_N2: the angle in which the

leaving group is ejected with respect to the incoming group tells us immediately from which side the molecule has been approached.

The coordinate system in which the collision is uniquely described is the center of mass system. Here, the total center of mass is at rest and therefore the momenta before and after the collision sum up to zero. Henceforth, the letter u will be used for velocities in the center of mass frame and the letter v for velocities in the laboratory fixed frame (see figure 3). The following equations can be easily derived:

$$v_{cm} = \frac{m_{r1}}{M} v_{r1} + \frac{m_{r2}}{M} v_{r2}; v_{rel} = v_{r1} - v_{r2} = u_{r1} - u_{r2}; v = u + v_{cm} \tag{10}$$

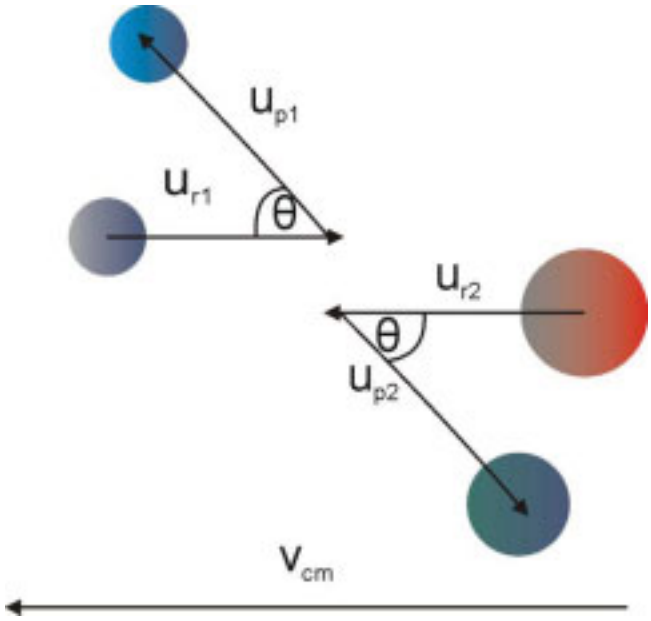

FIG. 3: Reactive scattering in the center of mass system

It should be noted that the connection to classical chemical kinetics can be seen by looking at equation 8 if σ is replaced by σ_r. Then the rate constant for a fixed relative speed is given by $k(v_{rel}) = \sigma_r(v_{rel}) \cdot v_{rel}$ and the thermal rate constant by the expectation value over the Maxwell-Boltzmann distribution: $k(T) = < \sigma_r v_{rel} >$. For a deeper and more detailed description of the subject of reactive scattering, the reader is referred to reference 16.

In this thesis a technique to measure the quantum state selective differential reaction cross section in only one molecular beam will be presented. The usual way to approach this

problem is the PHOTOLOC technique.[17] This uses two lasers which are superimposed in time and space, one to photolyze an adequate precursor and the other to state selectively ionize the products from the reaction of the photoproduct with another reactant present in the same molecular beam using REMPI spectroscopy. Since PHOTOLOC is subject to certain limitations concerning the speed distribution of the photolysis of the precursor and that of the products and is thus not generally applicable, we use a variation of the experimental configuration where the two laser beams are shifted in time and space. For this it would be ideal if the reaction would only take place in the volume of the detection laser which is of course not the case. This leads to strong bias with respect to the center of mass velocity in the detection of the reaction products. Therefore, the experiment has to be thoroughly modeled in order to be able to reconstruct the center of mass distribution. The reconstruction will be discussed together with the experimental results, so here I will describe the general modeling of the experiment which will be used to calculate certain probabilistic properties needed in the analysis in chapter 4.2.

The general problem can be written as follows:

$$\begin{aligned} I(\vec{v}) &= \int K(\vec{v},\vec{u},\vec{v}_{cm},t_r,t_D) I(\vec{u}) d\vec{u} d\vec{v}_{cm} dt_r dt_D + N_{\vec{v}} \\ &\propto \int P(\vec{v},\vec{v}_{cm},t_r,t_D|\vec{u}) P(\vec{u}) d\vec{u} d\vec{v}_{cm} dt_r dt_D + N_{\vec{v}} \end{aligned} \tag{11}$$

Equation 11 states that the measured intensity $I(\vec{v})$ for a certain laboratory velocity $\vec{v}$ is given by integration over the desired intensity of center of mass velocities $\vec{u}$ and a kernel function $K(\vec{v},\vec{u},\vec{v}_{cm},t_r,t_D)$ which is dependent on the laboratory velocity $\vec{v}$, the velocity in the center of mass system $\vec{u}$, the velocity of the reactant being the product of the precursor photolysis through $\vec{v}_{cm} = \vec{v}_p \cdot m_p / M$ (M: total mass, index p: photolysis product), the time t_r at which the reaction occurs and the time t_D at which the product is detected (given by the laser pulse length and the delay time). N_v denotes random noise. $I(\vec{v})$ is proportional to the integral over the probability density of the velocities in the center of mass system $P(\vec{u})$ weighted by the conditional probability $P(\vec{v},\vec{v}_{cm},t_r,t_D|\vec{u})$ that the product detected at t_D has the laboratory velocity $\vec{v}$ and was generated in a collision at the time t_r having the center of mass velocity $\vec{v}_{cm}$ (i.e. a certain reactant velocity $\vec{v}_p$), given that the velocity in the center of mass system is $\vec{u}$. Here the notation P(A|B) has been used to indicate a conditional probability that A will occur if B is given. Note that the orientation of the center of mass system varies with the velocity vector of the photolysis product. The other reactant is assumed to be uniformly

distributed on the scale of the spatial shift between the two lasers. For the transformation of $\vec{u}$ into the laboratory, the following convention has been chosen: the z-axis of the cm system points in the direction of the photolysis product velocity. Thus, $\vec{u}$ must be rotated by the polar angle θ_r about the y-axis and by the azimuthal angle φ_r about the laboratory z-axis. The angles are given by the reactant velocity $\vec{v}_p$ which is defined in the laboratory frame. Since the rotation about the z-axis of the center of mass system has no meaning whatsoever, it is left out. This has the effect that the u_x and u_y axes become different in this treatment (e.g. if the detection laser is shifted in the z-direction with respect to the dissociation laser, the positive u_x-axis is like the dark side of the moon never facing towards the detection laser). However, this effect is considered in the reconstruction to follow and since they have no meaning of their own, integration of the angel in the u_x,u_y-plane is carried out anyway. The situation is sketched in figure 4 for two different solid angles. The laboratory coordinate system is defined as follows: The x-axis lies in the direction of the laser beams, the z-direction in the direction of the TOF spectrometer (vide infra) and the y-axis is perpendicular to the x,z-plane. According to this model, the u_y component remains in the x,y-plane of the laboratory system.

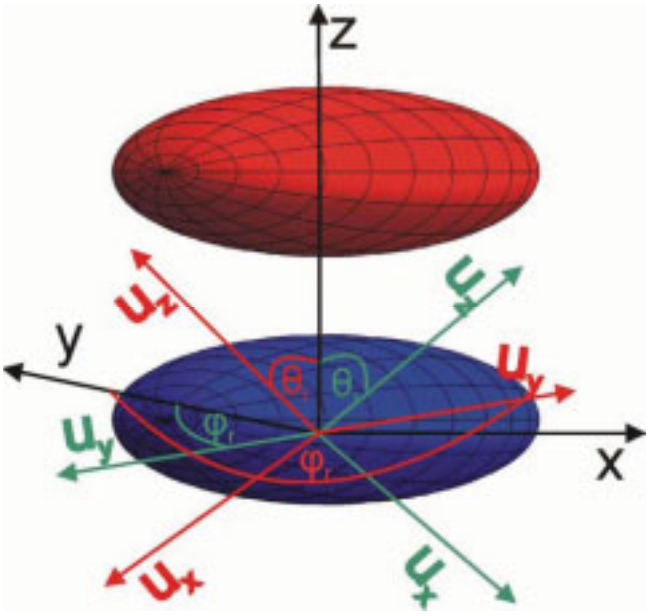

FIG. 4: Laboratory and center of mass system: first the rotation about the u_y/y-axis about θ_r is conducted, then rotation about the z-axis about φ_r. Two different situations are depicted in order to demonstrate the behavior of the u_x-axis. The dissociation volume is displayed in blue, the detection focus volume in red.